UM-P-96/53

AU9715875

ATOMIC RESOLUTION IMAGING OF FERROELECTRIC DOMAINS

L.A. BURSILL

School of Physics, University of Melbourne, Parkville, 3052, Vic., Australia

Electron optical principles involved in obtaining atomic resolution images of ferroelectric domains are reviewed, including the methods available to obtain meaningful interpretation and analysis of the image detail in terms of the atomic structures. Recent work is concerned with establishing the relationship between the essentially static chemical nanodomains and the spatial and temporal fluctuations of the nanoscale polar domains present in the relaxor class of materials, including lead scandium tantalate (PST) and lead magnesium niobate (PMN). Correct interpretation of the images required use of Next Nearest Neighbour Ising model simulations for the chemical domain textures upon which we must superimpose the polar domain textures; an introduction to this work is presented. A thorough analysis of the atomic scale chemical inhomogeneities, based upon the HRTEM results, has lead to an improved formulation of the theory of the dielectric response of PMN and PST, which is capable to predict the observed frequency dependence. Thus we now have an imaging tool (HRTEM) which may be combined with solid state and statistical physics principles to provide a deeper understanding of structure/property relationships.

INTRODUCTION

Imaging of ferroelectric domains requires some elaboration of the electron optical techniques, since we are often dealing with relatively weak departures from the normal non-ferroelectric state. This may require the use of many-beam dark-field imaging techniques as well as sophisticated image processing. High-resolution imaging of ferroelectric materials sometimes poses special problems due to specimen charging and specimen-induced astigmatism which results from the perturbing effects of local electrostatic fields. Our structural studies of a number of classical ferroelectric domain wall configurations have already been reviewed[1-3].

The principles and practice of HRTEM imaging have been thoroughly documented, see e.g.[4-6]; some extensions of the technique required for the detection of weak symmetry elements have been discussed[7-8]. The following is a brief introduction to HRTEM imaging leading to some recent applications.

A parallel beam of high-energy electrons is passed through a specimen less than 50nm thick. The transmitted and diffracted beams are collected by the objective lens and finally used to form a magnified image of the atomic structure. Typically the image may be digitized using a CCD-TV camera, allowing for some on-line or off-line image processing (Fig.1a). The instrument may also be capable of energy dispersive analysis of X-rays emitted by the specimen and/or electron energy-loss spectroscopy of electrons transmitted through the specimen (Fig.1b).

Provided the specimen in thin enough and certain electron optical conditions are met, then it may be possible to directly image the columns of atoms lying parallel to the incident beam. Thus a two-dimensional projection of the atomic structure along a principal zone axis of a crystal is the primary result. For example Fig.2 shows the [001] projection of a

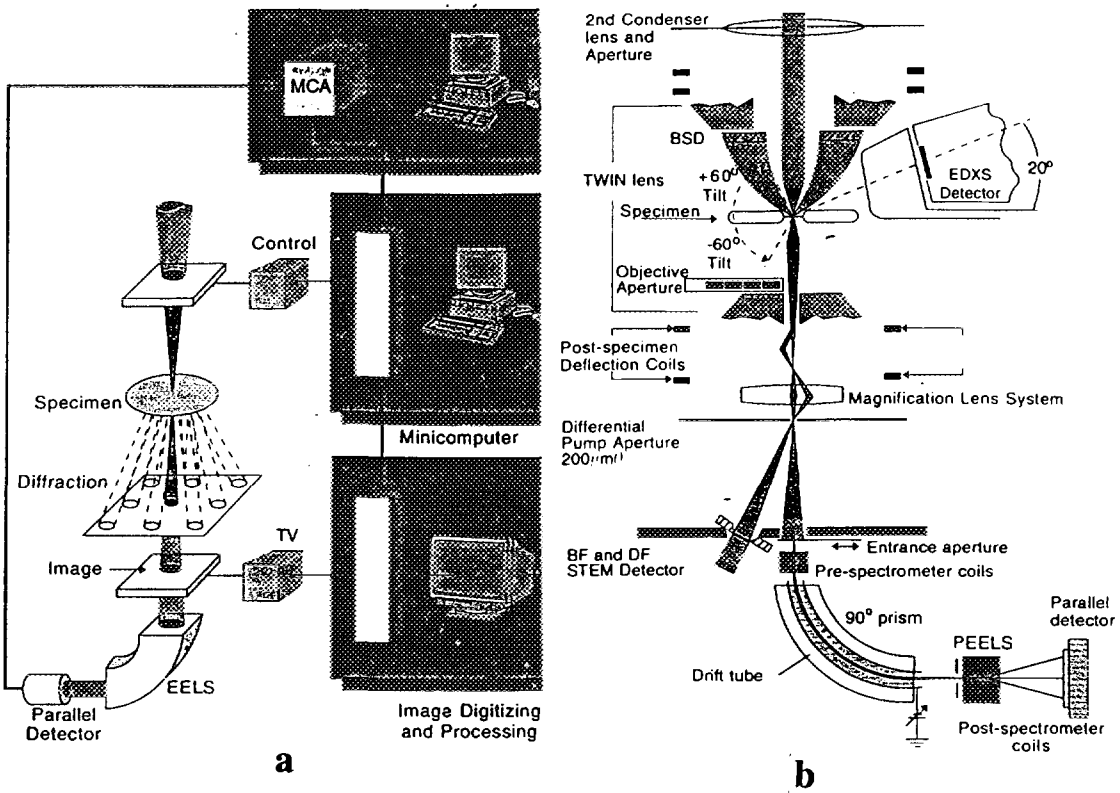

Figure 1: Typical lens and detector configurations used for HRTEM and analysis (a) HRTEM with CCD TV-camera and parallel electron energy loss spectroscpy (PEELS) (b) Side-entry goniometer with energy dispersive X-ray spectroscopy (EDX S, back-scattered electron detector (BSD), bright- and dark-field STEM detectors and PEELS

barium sodium niobate (BNN) having structure related to the tetragonal-tungsten bronze-type. Note the cations of this projection of the structure (inset) are visualized as black spots[9].

Complications arise if the crystal becomes too thick (greater than 10nm say), if the specimen and/or instrumental alignments are not precise (better than 0.1mRad say), if the specimen moves more than 0.1nm during the couse of the exposure or if the specimen becomes damaged during observation in the electron beam. Definitive image analysis is made using image-matching techniques based on computer simulations (see[4,5] for the theory and[4,6,7] for reviews of both experiment and theory of the HRTEM image matching techniques.

EXPERIMENTAL TECHNIQUES

Instrumental

HRTEM images may be obtained using e.g. a JEOL-4000EX or Philips CM-30 electron microscope operating at 100-400 kev; the spherical aberration coefficient of the ultra-high resolution pole-pieces is typically Cs=0.90-1.2 mm and the effective or interpretable image resolution is 0.17-2.3 nm. The specimen height is carefully adjusted to an optimum focussing current, when the objective lens astigmatism as well as the optical alignment parameters are set precisely against calibrated values.

The usual imaging condition is known as many-beam bright-field, when the crystal is oriented exactly along a principal zone axis of the crystal and the transmitted beam plus all

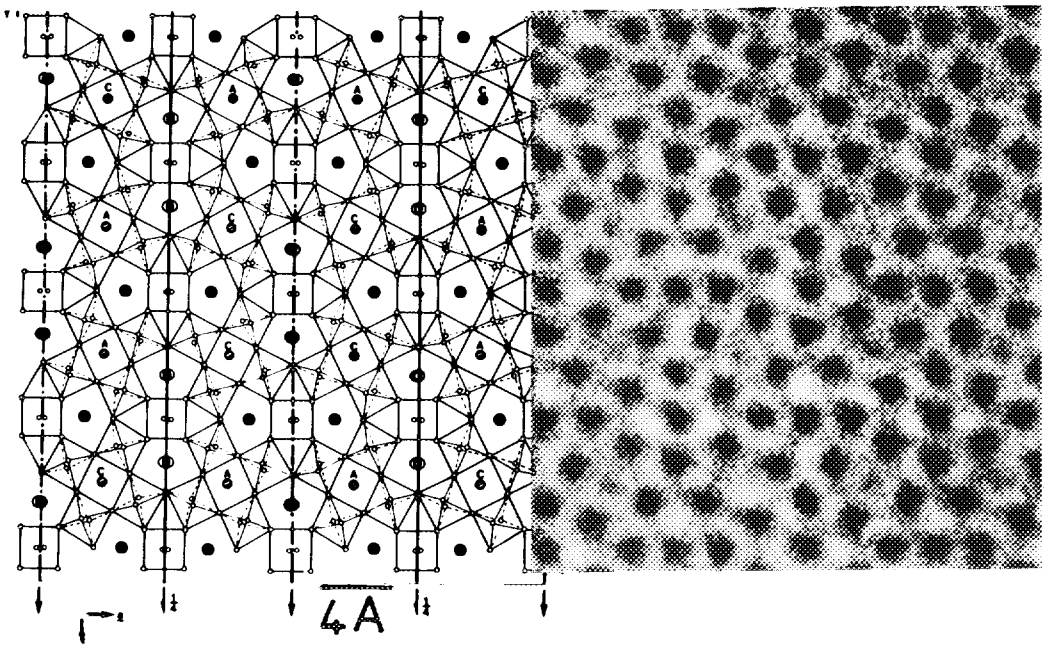

Figure 2: HRTEM image of barium sodium niobate; note correspondance between black spots and the cation positions,

diffracted beams scattered out to some angle α are accepted by the objective aperture and combine to form the image (Fig.3a). In some cases it is advantageous to use many-beam dark-field images (Fig.3b) or single beam bright- or dark-field images (Figs.3c,d). It will be shown below that image-processing techniques may be used to recover specific many or single beam bright-and dark-field images, starting with one high quality many-beam bright-field image.

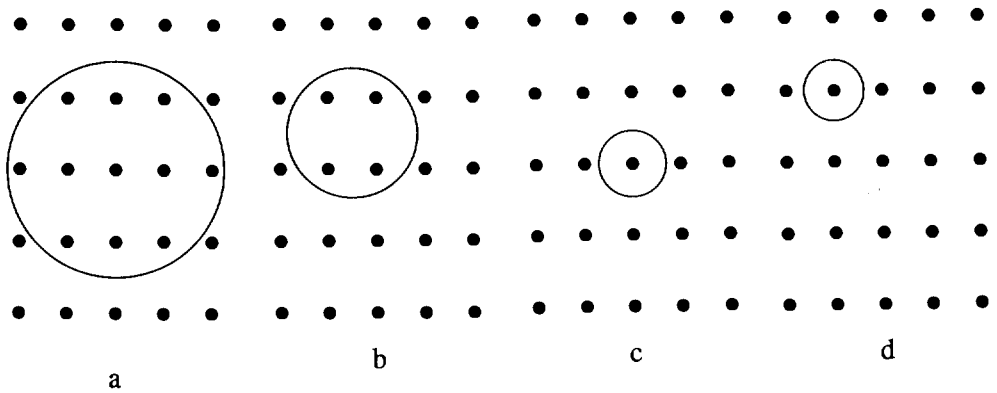

Figure 3: Illustrating the beams included in the objective aperture for (a) many-beam bright-field, many-beam dark-field, single beam bright-field (c) and single-beam dark-field.

Specimen preparation For best results it is recommended that wedge-shaped thin specimens be prepared by a dry method, such as fracture and mounted on copper grids with a minimum of adhesive; if necessary ion-thinned sections or cross-sections may be used or powdered specimens may be mounted on holey-carbon films after dispersion in a liquid. However ion-thinning tends to introduce amorphous surface layers and solvents or hydroxyl ions tend to enhance electron irradiation damage effects on the specimen; both of these effects may detract from the availability of high quality, interpretable HRTEM images.

Image simulations

HRTEM simulations are usually based on the physical optics approach to electron diffraction and imaging[4,5]. All the non-linear N-beam dynamical scattering, as well as lens aberrations and Fresnel propagation effects of the objective lens are included. Periodic continuation methods, as developed for atomic resolution images[10,11] were obtained using MEDIS (Melbourne Electron Diffraction and Image Simulation) software, most recently due to Fan and Peng. There are several HRTEM image simulation packages available, see e.g. information supplied by various groups available at www sites such as
http://www.ph.unimelb.edu.au/groups.html or
http://cimewww.epfl.ch/
The aim of the simulations is to obtain semi-quantitative image-matching of experimental and calculated images, assuming some detailed atomic model proposed for the structure. This finally requires that the specimen thickness and the objective lens defocus values be determined to better than 1 nm and that the lens aberrations coefficients are also known to about 5%. Model sensitivity varies according to the atomic numbers and spacings involved, as well as crystal orientation; this must be determined on a case by case basis. Thus for perovskite-related lead scandium tantalate it is possible to obtain both B-site occupancies and A-site cation shifts[12], as shown in Fig.4.

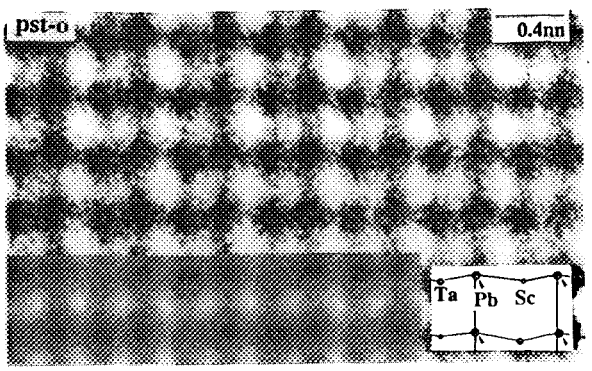

Figure 4: HRTEM simulations and experimental images for lead scandium tantalate.

Image processing

For the case of 1:1 ordered nanodomains in lead magnesium niobate (PMN) we used Monte Carlo methods to obtain Next-Nearest-Neighbour-Ising model simulations to represent the B-site cation distributions[13]. It was necessary to include electrostatic interactions to limit the size of the 1:1 ordered regions. We wanted to determine the latter by comparison with experimental HRTEM images. However the experimental images from thin edges of the specimens showed little evidence for the chemical domain structures. We therefore developed the following image-processing technique in order to reconstruct various single- and many-bean bright- and dark-field images, which have allowed the domain size to be determined. Further details of the methods may be found in the paper by Fan et al[11].

Fig.5a is a digitized experimental image of PMN whereas Fig.5b shows a computer simulated image of the NNNI model after 2000 Monte Carlo steps; insets show the corresponding power spectra, which represent the electron diffraction patterns which would be obtained from Figs.5a,b. Figs.5b,f show the corresponding many-beam bright-field images obtained using the filters shown (see insets). Nore that the image reconstructions

were made using the real and imaginary parts of the Fourier transforms. Actually, Fig.5b shows the real part of the Fourier transform of a set of h+1/2, j+1/2, k+1/2 superlattice beams plus the transmitted beam. Note that the NNNI model provides a reasonable representation of the processed experimental image (Fig.5b).

Figs.5c,g are the corresponding high resolution many-beam dark-field images retrieved from the experimental and NNNI models respectively, using four h+1/2, j+1/2, k+1/2 superlattice beams. Finally, Figs.5d,h show single beam dark-field images obtained using a single h+1/2, j+1/2, k+1/2 superlattice beam. Again, the NNNI model is in good agreement with the processed experimental image. Note that the experimental image was carefully chosen to correspond to a very thin area, probably less than 3 nm thick; in this case there is a one-to-one correspondance between the computer simulated images and structures and the experimental images. As the crystal thickness increases the relationship between image intensity and the structures being imaged quickly becomes non-linear; the prediction of the thicker crystal images and image reconstructions may be followed using the multislice methods, but space does not permit further discussion. Prior to the above results, many authors have made the simplistic assumption that a bright spot in the single beam dark-field image, obtained using a superlattice reflection, represented the diameter of the 1:1 ordered domains in PMN; clearly this is can only be true for extremely thin crystals, when there is no projection overlap.

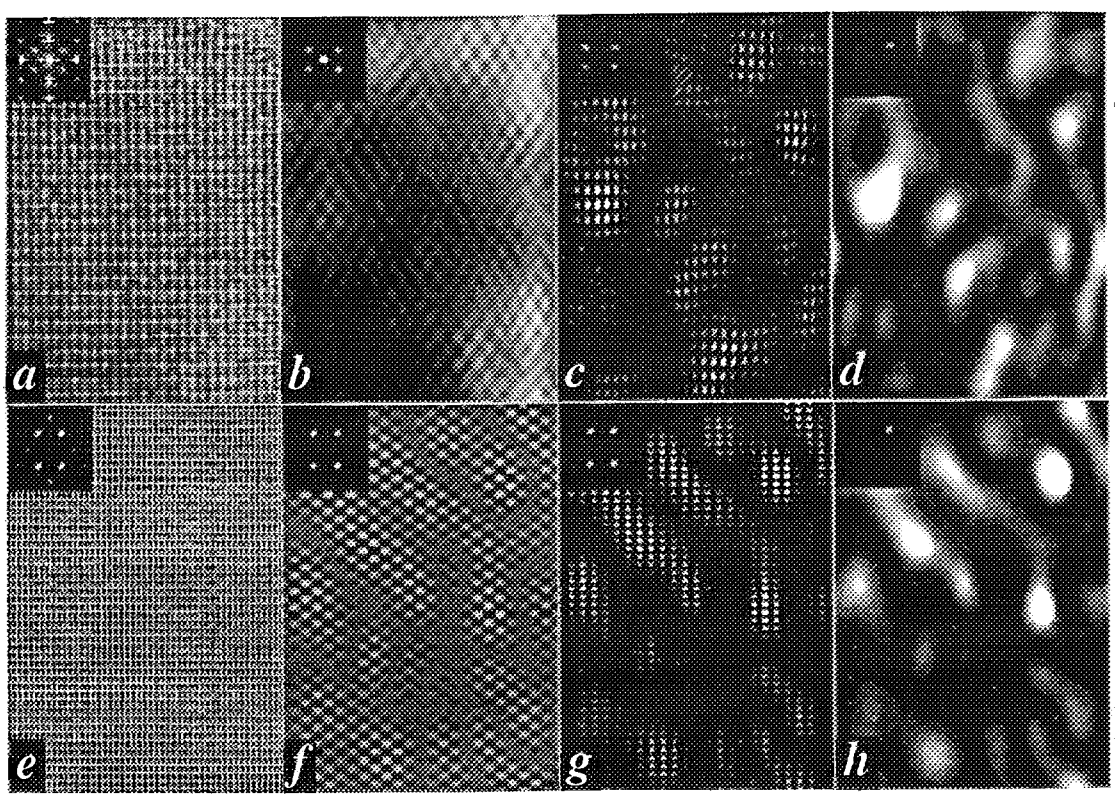

Figure 5: (a) Digitized image of experimental image of PMN; (e) computer simulated image of PMN; (c-h) show details of the image reconstructions referred to in detail in the text; insets are power spectra.

Polar domains may be observed using dark-field images from reflections such as 111 for PMN or PST; Fig.6 shows a time sequence of an area of PST, showing low frequency (1-15HZ) polar fluctuations at room temperature on the scale of about 5nm.

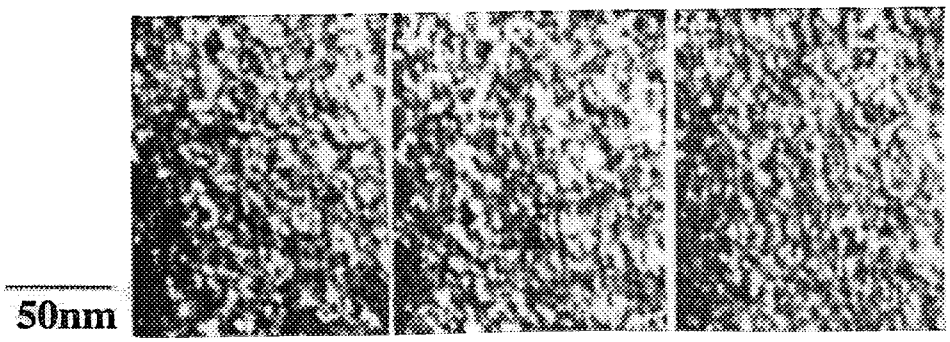

Figure 6: Polar domain fluctuations in PST on the 5nm scale at room temperature.

CONCLUSION

HRTEM bright- and dark-field imaging techniques have a vital and interesting role to play in exposing chemical nanodomain textures. We are now going through the process of overlaying polar domain textures onto the chemical nanodomains; Potts model simulations, using the above NNNI model simulations as starting point to generate the local electric field distributions associated with charged chemical defects, have allowed us to predict the evolution of the polar domains in PMN and PST as a function of temperature. We used these results to predict the temperature and frequency dependence of the dielectric response of PMN and PST[14,15]. It remains to apply image-processing techniques similar to those described above to obtain experimentally both the chemical and polar domain structure from the one set of HRTEM images. Note that this may only be done for any static or relatively low frequency temporal fluctuations of the polar domain states[12].

ACKNOWLEDGEMENTS

This work was supported financially by the Australian Research Council. The author is grateful for the support of Peng Julin, Qian Hua and Fan Xudong.

REFERENCES

1. L.A. Bursill and Peng, J.L., *Ferroelectrics*, **70**, 191-203 (1986).
2. J.L. Peng and L.A. Bursill, *Phase Transitions*, **34**, 171-188 (1991).
3. L.A. Bursill and J.L. Peng, *Key Engineering Materials*, **66/67**, 421-460 (1992).
4. J.M. Cowley, *Diffraction Physics*, North-Holland, N.Y. (1989).
5. P. Goodman and A.F. Moodie, *Acta Crystallogr.A*, **30**, 280-289 (1974).
6 J.H.C. Spence, *Experimental High-Resolution Electron Microscopy*, O.U.P (1991).
7 L.A. Bursill, *Ultramicroscopy*, **18**, 1-10 (1985).
8. L.A. Bursill and J.L. Peng, *Ultramicroscopy*, **18**, 235-240 (1985).
9. J.L. Peng and L.A. Bursill, *Acta Crystallogr. B*, **43**, 504-512 (1987).
10. D.S. MacLagen, L.A. Bursill and A.E.C. Spargo, *Philos. Mag.*, **35**, 757-780 (1977).
11 X.D. Fan, H. Qian, J.L. Peng and L.A. Bursill, *Integr. Ferroel.*, **9**, 233-242 (1995).
12. L.A. Bursill, J.L. Peng, H.Qian and N. Setter, *Physica B*, **205**, 305-326 (1995)
13. L.A. Bursill, H. Qian, J.L. Peng and X.D. Fan, *Physica B*, **216**, 1-23 (1995).
14. H. Qian, Ph.D Thesis, University of Melbourne (1996).
15. H.Qian and L.A. Bursill, *Phys. Rev. B*, in press (1996).